UCSF

Title

Motor System Interactions in the Beta Band Decrease during Loss of Consciousness

Permalink

Journal

Journal of Cognitive Neuroscience, 28(1)

ISSN

0898-929X

Authors

Swann, Nicole C
de Hemptinne, Coralie
Maher, Ryan B
et al.

Publication Date

2016

DOI

10.1162/jocn_a_00884

Peer reviewed

Motor System Interactions in the Beta Band Decrease during Loss of Consciousness

Nicole C. Swann[1,*], **Coralie de Hemptinne**[1], **Ryan B. Maher**[3], **Catherine A. Stapleton**[4], **Lingzhong Meng**[2], **Adrian W. Gelb**[2], and **Philip A. Starr**[1]

[1] Department of Neurological Surgery, University of California San Francisco, 94143

[2] Department of Anesthesia and Perioperative Care, University of California San Francisco, 94143

[3] Fidere Anesthesia Consultants, 94040

[4] Alta Bates Summit Medical Center, 94705

Abstract

Communication between brain areas and how they are influenced by changes in consciousness are not fully understood. One hypothesis is that brain areas communicate via oscillatory processes, utilizing network-specific frequency bands, that can be measured with metrics that reflect between-region interactions, such as coherence and phase amplitude coupling (PAC). To evaluate this hypothesis, and understand how these interactions are modulated by state changes, we analyzed electrophysiological recordings in humans at different nodes of one well-studied brain network: the basal ganglia-thalamo-cortical (BGTC) loops of the motor system, during loss of consciousness induced by anesthesia. We recorded simultaneous electrocorticography (ECoG) over primary motor cortex (M1) with local field potentials (LFPs) from subcortical motor regions (either basal ganglia or thalamus) in 15 movement disorder patients during anesthesia (propofol) induction as a part of their surgery for deep brain stimulation. We observed reduced coherence and PAC between M1 and the subcortical nuclei, which was specific to the beta band (~18-24 Hz). The fact that this pattern occurs selectively in beta underscores the importance of this frequency band in the motor system, and supports the idea that oscillatory interactions at specific frequencies are related to the capacity for normal brain function and behavior.

Keywords

Electrocorticography; Local Field Potentials; Consciousness; Motor Cortex; Basal Ganglia-Thalamo-Cortical Loops; Electrophysiology

Introduction

How do functionally related brain areas communicate over long distances? One hypothesis is based on oscillatory synchronization in specific frequency bands, usually lower than ~50 Hz (Siegel et al., 2012). Coherence is a simple measure of oscillatory synchronization that

[*] Corresponding Author Health Sciences East, Rm # 823, 513 Parnassus Avenue, San Francisco, CA 94143, ; Email: Nicole.Swann@ucsf.edu

may support long-distance neural interactions. It reflects interactions between brain areas related to the consistency of the phases and amplitudes of their neuronal signals (Fries, 2005). On the other hand, higher frequency, broad-band, activity ("broadband gamma", 70-250 Hz) seems to reflect local neural activity (Miller et al., 2007, Manning et al., 2009). Canolty and colleagues demonstrated that, in some instances, broadband gamma amplitude is modulated by the phase of lower frequency oscillatory rhythms (Canolty et al., 2006). This phase amplitude coupling (PAC) provides a mechanism that could explain how low frequency oscillatory changes, which are well suited to coordinate activity over long distances, can influence local neuronal activity (Fries, 2005, Canolty and Knight, 2010). When PAC is calculated from the phase and amplitude of signals recorded from two different brain areas, it may also reflect interactions between brain regions.

Transitions in consciousness afford an opportunity to evaluate how these basic measurements of brain interactions change in the context of profound behavior/state changes. While the underlying causal mechanisms of consciousness remain unclear, there is converging evidence that transitions of consciousness are characterized by a change of network dynamics wherein local brain networks become more isolated from one another, disrupting the brain's ability to integrate information (Alkire et al., 2008, Lewis et al., 2012). Since all but the most basic forms of behavior are only possible in the conscious state, we hypothesized that the most functionally important network interactions are only present in the conscious state. To better understand how those interactions might mediate behavior, and perhaps relate to communication in brain networks, we sought to study how simple metrics of brain interactions (coherence and PAC) in the motor system change during anesthesia-induced transitions in consciousness.

To address this goal, we combined electrocorticography (ECoG) and subcortical local field potential (LFP) recordings in movement disorder patients undergoing surgical implantation of deep brain stimulation (DBS) leads (de Hemptinne et al., 2013, de Hemptinne et al., 2015). This approach provides a unique opportunity to acquire field potential data from functionally related cortical and subcortical structures (primary motor cortex (M1) and motor territories of the basal ganglia and thalamus). Because DBS targets vary across individuals/diagnoses, we have the opportunity to sample from a number of different subcortical nodes in the basal ganglia-thalamo-cortical (BGTC) loop (although this does increase variability in our sample). The BGTC circuit is particularly well suited to address questions concerning network interactions because structural connectivity in the motor loop is relatively well defined, with connections from cortex to basal ganglia to thalamus and then back to cortex (Alexander et al., 1986). Additionally, the electrophysiological signatures in the motor system have been studied extensively. The beta frequency range (13-30 Hz) dominates and is dynamically modulated during movement (Pfurtscheller, 1981, Murthy and Fetz, 1992, Sanes and Donoghue, 1993, Crone et al., 1998b, Cassidy et al., 2002, Brovelli et al., 2004, Kuhn et al., 2004). We hypothesized that loss of consciousness would be characterized by reduced interactions between cortical and subcortical regions, measured with coherence and inter-region PAC, and that this would be particularly prominent in the beta frequency band.

Methods

Patients

Fifteen patients (4 females/11 males, average age 62 years) were recruited from the Surgical Movement Disorders Clinic at the University of California, San Francisco (UCSF). Patients were scheduled to undergo surgery to implant a permanent subcortical DBS lead to treat their movement disorders. All patients were simultaneously participating in a study of the contribution of cortical oscillatory activity to movement disorders pathophysiology, using ECoG from a subdural strip array inserted through the standard frontal burr hole used for DBS insertion, and temporarily placed over the primary motor cortex (Crowell et al., 2012, de Hemptinne et al., 2013, Shimamoto et al., 2013). Our standard surgical procedure requires that patients be awake for microelectrode mapping and DBS lead insertion, followed by anesthesia induction (for wound closure). This procedure provides the opportunity for brain recording during anesthesia-induced loss of consciousness, avoiding the need to administer anesthetics solely for research purposes.

The goal of the present study was to examine interactions between nodes of the motor system during loss of consciousness, rather than focusing on a specific movement disorder. Therefore, we included patients with varying diagnoses and varying subcortical targets within the motor network to enable the identification of network motifs common to changes in consciousness independent of disease state. Twelve of the patients had Parkinson's disease (PD), two had Essential Tremor (ET), and one had primary Dystonia. Four PD patients had DBS leads placed into the globus pallidus interna (GPi) while the other eight had subthalamic nucleus (STN) leads, with target choice dictated by clinical criteria (Follett et al., 2010). The DBS target for ET patients was the ventrolateral thalamus. The target for the dystonia patient was GPi. The study methodologies were approved by the institutional ethics committee and are in agreement with the Declaration of Helsinki. All patients provided written informed consent to participate in the study, and the use of a temporary cortical ECoG array placed for research purposes was an explicit part of the consent discussion.

ECoG Strip Placement—ECoG was recorded from one hemisphere during the surgery. For patients receiving unilateral DBS, the ECoG was placed ipsilateral to the side of the DBS. For patients receiving bilateral surgery, the side of the ECoG was determined based on the clearest anatomic demarcation of the central sulcus on preoperative magnetic resonance imaging (MRI). Eleven patients had left side recordings, while four had right.

The data from the dystonia patient and 5 PD patients were collected with a 6 electrode ECoG grid (1 cm spacing between electrodes, see **Figure 1A**), and the other 7 PD patients and both ET patients were recorded with a 28-electrode ECoG strip (4 mm spacing between electrodes, see **Figure 1B**). The type of ECoG strip used depended on the parent study of movement disorders physiology, since during this study period we transitioned from the lower spatial resolution recording to a higher resolution technique. Each strip was placed with at least one electrode covering M1. The intended target location for the center of the ECoG strip was the arm area of M1, 3 cm from the midline and slightly medial to the hand knob (Yousry et al., 1997). Adequate localization of the ECoG strip was confirmed using

either preoperative MRI merged to an intraoperative CT (13 subjects) or using intraoperative lateral fluoroscopy with a radio-opaque marker placed on the skin indicating the intended target in M1 that was visible relative to the electrode strip (2 subjects), as previously described (Crowell et al., 2012, de Hemptinne et al., 2013, Shimamoto et al., 2013, de Hemptinne et al., 2015). In all subjects functional localization was also examined using somatosensory evoked potentials (SSEPs, frequency = 2 Hz, pulse width = 200 μs, pulse train length = 160, amplitude = 25-40 mAmp), as has been previously reported (Crowell et al., 2012, de Hemptinne et al., 2013, Shimamoto et al., 2013). Note that for the 28-electrode strip, there were two rows of 14 electrodes (see **Figure 1B**), so it was expected that 2 electrodes localized immediately anterior to the central sulcus would show a phase reversal relative to the post-central sulcus electrodes.

DBS Electrode Implantation

Anatomic targeting of the desired subcortical structure was performed as previously described (Starr et al., 2002, Papavassiliou et al., 2004, Starr et al., 2006). For the GPi and STN targets, the proper location was verified by eliciting movement-related single cell discharge patterns (Starr et al., 2002). For all regions, the correct placement was verified by test stimulation, as well as intraoperative fluoroscopy (all patients), intraoperative CT (13 patients) (Shahlaie et al., 2011), and post-operative MRI (all patients).

Consciousness Assessment and Anesthesia Parameters

Continuous recordings were taken after DBS placement, but prior to burr hole closure and DBS pulse generator placement, while the patients were slowly anesthetized with propofol. Data from PD patients were recorded after at least 12 hours off antiparkinsonian medications. Consciousness was assessed every 3 minutes using the Modified Observers Assessment of Alertness/Sedation Scale (MOAA/S, see Table 1, Chernik et al., 1990). Ratings were recorded by an anesthesiologist (AG, LM). When the clock started for the assessment session (time zero), a button was pressed which generated a voltage deflection in an auxiliary channel digitized with the electrophysiology data. This synchronized the times noted by the anesthesiologist with the electrophysiology data.

Anesthesia induction with propofol was performed slowly with the goal of achieving an estimated plasma level (Marsh Model) of 4 mcg/ml at approximately 15 minutes (Smith et al., 1994). Induction ended when all patients no longer responded to painful stimulation according to MOAA/S scale (see **Table 1**). Propofol sedation had also been used during the drilling of the burr holes prior to intracranial recording, but was stopped for subcortical mapping and DBS lead testing, at least 60 minutes prior to initiating the recordings analyzed here. This is ample time for the effects of propofol to wear off (Fechner et al., 2004, Raz et al., 2010).

ECoG and LFP Recordings

ECoG recordings were performed using either the Alpha Omega Microguide Pro, Alpha Omega, Inc (for the 6 electrode strip, **Figure 1A**) or the Tucker Davis Technologies Recording System (for the 28 electrode strip, **Figure 1B**). For the Alpha Omega system data were sampled at 3000 Hz. Data from each of the 5 more posterior electrodes were

referenced to the most anterior electrode. A needle electrode in the scalp served as the ground. Data were band-pass filtered at 1-500 Hz. For the Tucker Davis System, data were sampled at 3051 Hz. All electrodes were referenced to a scalp needle electrode that also served as the ground. Data were low pass filtered at 1500 Hz. Since there was no high pass filter applied during data acquisition, the mean of each electrode was subtracted during offline preprocessing to detrend the data. See **Figure 2A** for an example of the raw ECoG data.

LFP recordings were from the subcortical target ipsilateral to ECoG placement were recorded in a bipolar configuration from the middle two cylindrical contacts (1.5 mm height, 1.2 mm diameter) of a quadripolar lead (Medtronic model 3389, 0.5 mm between contacts, 8 patients or Medtronic model 3387, 1.5 mm between contacts, 7 patients), with electrode 1 as the active and electrode 2 as the reference. The guide tube for the DBS lead served as ground. For the 6 patients for whom the 6-electrode cortical strip was used, the LFP recordings were done with the Alpha Omega system using the same Alpha Omega parameters described above for ECoG. For all the PD patients who were tested with the 28-electrode strip, LFP data was still collected using the hardware from the Alpha Omega system (which was necessarily present as it is FDA approved for clinical micro-electrode recordings for mapping), however the analog signal was streamed to the Tucker Davis system and digitized there at 25,000 Hz sampling rate and then subsequently down-sampled. For the sessions with ET patients, the Alpha Omega system was not present in the room, as micro-electrode recordings were not used for ET. Thus, LFPs were recorded in the same manner as the ECoG electrodes (data from electrode 1 and 2 of the DBS electrode were both recorded with the needle electrode as the reference and ground), and then subsequently referenced in a bipolar configuration offline. See **Figure 2B** for an example of the raw LFP data.

Electrophysiological Pre-Processing

All data were initially down-sampled to 1000 Hz, and line frequency noise (at 60 Hz, 120 Hz, and 180 Hz) was removed using a third-order Butterworth notch filter which spanned a 4 Hz range centered at each frequency (i.e. 58-62 Hz for 60 Hz). Data were then re-referenced. For the 6 electrode strip a bipolar montage was used such that each electrode was referenced to the anterior electrode (C1-C2, C2-C3….). For the 28-electrode strip a common average reference was used including all ECoG electrodes (excluding any with obvious, continuous, noise). Each reference strategy is best suited for the given electrode configuration: an average reference montage is not appropriate when there are only 5 active electrodes to contribute to the reference, and a bipolar reference is less optimal for the 28 electrode strip with small contacts and very close spacing. To determine if the different referencing schemes influenced our results we re-ran our analyses using an average reference scheme for all subjects and the results were similar, thus this difference in analysis is unlikely to have strongly influenced our findings. Subcortical LFP electrodes were processed in the same way as above (down-sampled and filtered). All raw data were manually inspected and periods of artifact (e.g., electrical artifact caused by medical equipment or movement) were noted and excluded from analysis.

During data recording the anesthesiologist performed ratings every three minutes to assess the patient's level of consciousness (see Table 1). Data were assigned a consciousness rating according to the assessment at the end of each three-minute time segment. For instance, if after 3 minutes the anesthesiologist rated the patient's alertness as a 5 and at 6 minutes rated it as a 4, the segment of the electrophysiology data corresponding to 0-3 minutes would be marked as 'state 5' and times 3-6 minutes would be marked as 'state 4'. Not all patients were observed at each state. The longest artifact-free period of each state was used for analysis. On average this was 218.1 seconds, and was always greater than 31 seconds. Because both coherence and PAC can vary over time even without an overt change in behavioral state, we included the longest data segments possible for each subject and each level of consciousness. However, because coherence and PAC values can also be influenced by differences in the length of data analyzed, we conducted a control analysis to verify that differences in data length were not systematically driving our observed differences. In this analysis, for each subject, data of the same length from each state were used for comparison.

For each patient the cortical electrode(s) that most closely corresponded to M1 were selected based on both the anatomical localization and SSEP waveforms. This was done prior to examining the data from the anesthesia induction file. For the 28-electrode strip, there were two rows of 14 electrodes, so we selected one M1 electrode from each row that met these same criteria. In this case, power, coherence, and PAC (described below) were calculated separately for each of these electrodes and then averaged for each electrode pair. For the 6-electrode strip, the electrode selection procedure described above typically led to the selection of one electrode which clearly lay over M1 (at the border of the central sulcus and the pre-central gyrus), that also showed a clear SSEP phase reversal. For the 28-electrode strip, where the electrodes were smaller and spaced closer together, definitive selection of the two optimal M1 electrodes was less clear (regardless of reference scheme used). In order to test whether ambiguous selection of the M1 electrode may have influenced our results, we conducted a test wherein all electrodes on each strip were included in the analysis. (In this case, signal processing calculations described below were calculated for each electrode separately and then the final results were averaged, such that each subject contributed only one data point to the group statistics.) While this method clearly provides less spatial specificity, results were similar even when all electrodes were included. Thus, ambiguity in the selection of the optimal M1 electrode did not distort our results. The fact that results were similar for the M1 electrode and the entire strip most likely reflects the fact that the strip was placed to span precentral and postcentral gyri, which generate similar oscillatory signatures (Crone et al., 1998b).

Electrophysiological Signal Processing

All analyses used a combination of custom Matlab scripts and EEGLAB functions (Delorme and Makeig, 2004). We implemented two main types of analyses. First, we analyzed the activity of each area (M1 and the subcortical region) separately. We calculated power spectral density (PSD) and PAC (Canolty et al., 2006, Tort et al., 2008) within each region. Analyses for each patient, state, and region (M1 and subcortical) were calculated separately in Matlab.

PSD analysis used the Welch method (pwelch function in Matlab with a 512 ms window, 256 ms of overlap, see **Figure 2C and 2D** for an example of PSD in one subject). Statistics were then calculated based on the log PSD values. However, results were similar if non-log transformed values were used.

PAC was calculated using the "Kullback-Leibler (KL)-based modulation index" method, which has been previously described (Tort et al., 2008, de Hemptinne et al., 2013). In brief, the M1 ECoG and subcortical LFP signal were filtered separately using a two-way FIR1 filter (eegfilt with 'fir1' parameters). Low frequency signals were filtered individually at frequencies ranging from 2-50 Hz, with a 2 Hz bandwidth, and the phase was extracted from this signal using a Hilbert transform. Similarly, the amplitude of the high frequency broadband gamma signal was extracted by taking the Hilbert transform of the band-pass filtered data (70-150 Hz). Then, the distribution of the instantaneous amplitude envelope was computed for every 20° interval of the instantaneous phase (see Figure 2F). The coupling ("modulation index") between the phase of each low frequency rhythm and the high frequency amplitude was then determined by computing the entropy values of this distribution and normalizing by the maximum entropy value (Tort et al., 2008).

Second, we analyzed subcortical-cortical interactions by calculating coherence and cross-structure PAC. Analyses were performed for each subject and state separately, using signals from both the M1 ECoG and the subcortical LFP. We calculated coherence for frequencies ranging from 2-50 Hz, with a 2 Hz bandwidth, by filtering both the M1 ECoG and subcortical LFP using the same two-way FIR1 filter used to calculate PAC. Complex signals were then obtained for each filtered signal by taking the Hilbert transform. Coherence between the ECoG electrode(s) and the subcortical LFP was calculated using the corresponding auto-spectra (W_{xx} and W_{yy}) and cross-spectra (W_{xy}) of the filtered complex signals.

$$ Coh\,(f) \quad = \quad \frac{|W_{xy}\,(f)\,|}{\sqrt{W_{xx}\,(f)}\,\sqrt{W_{yy}\,(f)}} $$

Here x and y refer to data from the 2 regions (i.e. cortical and subcortical). W_{xy} was calculated by taking the sum over time of the complex signal of × multiplied by the conjugate of the complex signal of y. W_{xx} and W_{yy} were calculated as the sum over time of the amplitude of each (x and y) complex signal. See **Figure 2E** for an example of coherence at all frequencies in one patient.

Between-region PAC was calculated in the same way as within-region PAC described above, except that the low frequency phase component and the high frequency amplitude component were derived from signals from different brain regions (M1 ECoG and subcortical LFP). We examined PAC using both the phase of the subcortical LFP and amplitude of M1 ECoG and the opposite configuration. See **Figure 2F** for an example of PAC in one patient.

Statistical Analysis of Data Grouped Across Patients

For statistical comparisons of the change across patients during anesthesia induction a non-parametric paired sign-rank test was computed comparing, for each patient, the metric of interest (power, within region PAC, coherence, or between region PAC) for data corresponding to the state during which the patient was most awake (state 5, or closest to 5) to the data corresponding to the state during which the patient was most asleep (state 0, or closest to 0). This was done separately for each frequency. Results were then corrected for multiple comparisons (for all frequencies examined) using a false discovery rate (FDR) correction.

Results

Propofol and Monitoring Results

Each patient reached an "unconscious" state (i.e. MOAA/S value = 0 or 1). This was achieved on average in 22.5 minutes from the start of the file recording (SD = 8 minutes). For each patient a minimum of 3 anesthetic states were observed.

High Frequency Spectral Power Decreases and Low Frequency Power Increases in the Cortex and Subcortical Nuclei

The signal amplitudes were typical for ECoG and LFP data, with an average root mean square value for M1 of 56 microvolts for the most awake state, and 64 microvolts for the most asleep state (p<0.04, with a paired, sign-rank test). The subcortical LFP root mean square values were on average 8 microvolts (not significantly different for awake versus asleep, p > 0.15, **Figure 2**).

During induction the subcortical LFP was characterized by an increase in low frequency power (4-6 Hz, p<0.05, FDR corrected) and a decrease in higher frequency (broadband) activity (all frequencies 20-250 Hz, p<0.05, FDR corrected) (**Figure 3**). In the cortex, a similar pattern was observed for the low frequency power increase (2-6 Hz, p<0.05, FDR corrected) and high frequency decreases (144-250 Hz, but not all frequencies in this range were significant, p<0.05). However the decrease in high frequency power in the cortex was not significant when correcting for multiple comparisons (**Figure 4**). While the cortical high frequency effect was weak, previous ECoG work has shown similar cortical changes in these frequency ranges during propofol induction (Breshears et al., 2010, Verdonck et al., 2014). Thus, while our result was not statistically robust, it trends in the direction reported by others.

Of note, M1 beta power did not change with induction of anesthesia. While subcortical beta power did decrease during induction, this was a non-specific effect, since all frequencies above 20 Hz were reduced.

Coherence Between Cortex and Subcortical Nuclei Decreases During Induction

Across patients, there was a spectrally specific decrease in coherence in the beta band (18-24 Hz) during propofol-induced loss of consciousness (p<0.05, FDR corrected) (**Figure 5**). This occurred in the setting of no significant change in cortical beta power and a non-

specific decrease in power in all frequencies above 20 Hz in the subcortical LFP. The control analysis for which the same recording durations were used for both the "awake" and "asleep" epochs, produced similar results (significant decrease in coherence for 20-24 Hz, $p<0.05$ FDR corrected). Thus, variability in data length is not driving the observed effect.

We also examined the change in the phase of the beta coherence, and, though some patients showed a change, it was not consistent across patients (data not shown). Coherence patterns at other frequencies were variable across patients.

Phase Amplitude Coupling Between Cortex and Subcortical Nuclei Decreases During Induction

We calculated PAC in two ways. First we tested the within region PAC for M1 and the subcortical target separately, and did not observe any significant effects associated with anesthesia induction when correcting for multiple comparisons.

We then calculated inter-region PAC taking the phase from the subcortical target and the amplitude from the M1 ECoG and vice versa. With phase from the subcortical target and amplitude from the M1 ECoG, there was a significant decrease in PAC during induction, again in the beta band (18-20 Hz, $p<0.05$, FDR corrected, see **Figure 6**). The control analysis for which the same recording durations were analyzed for both the "awake" and "asleep" epochs produced similar, though slightly weaker results (significant decrease in inter-region PAC for 18-20 Hz, $p<0.05$, uncorrected). Thus variability in data length is unlikely to be driving the observed effect.

Results in other frequency ranges were variable across subjects. Calculating the PAC using the cortical phase and subcortical amplitude revealed no significant results associated with anesthesia induction.

Discussion

To evaluate changes in interactions between connected brain regions of the motor network associated with loss of consciousness, we collected multi-site field potential recordings from structures in the motor network in 15 subjects undergoing DBS surgery, and examined changes in oscillatory activity. We found a decrease in interactions, measured with coherence and inter-region PAC, between brain regions in BGTC loops during loss of consciousness, specific to the beta band. Importantly, the beta frequency band was the only band to have a consistent change in between-structure coherence and PAC across subjects, and this was not the case for cortical or subcortical spectral power. We also observed a decrease in broadband gamma activity in the subcortical nuclei and a similar, though weaker, decrease in cortex. This was accompanied by an increase in low frequency power in both cortex and subcortical nuclei.

Throughout the brain cortical structures communicate with functionally homologous subcortical modulators, and this communication is thought be mediated in part by synchronization in oscillatory activity. The motor system represents one such pair, with well-characterized anatomic connections from cortical motor areas to basal ganglia and thalamus

(Alexander et al., 1986), and robust oscillatory activity that is predominantly in the alpha or beta range (Pfurtscheller, 1981, Crone et al., 1998b, van Wijk et al., 2012). Our focus on the motor system was motivated by the fact that it can be ethically studied using invasive electrophysiological methods during DBS surgery. We expect that the motor system is a reasonable model for other brain networks, and that some of the observed patterns may be generally applicable, with network-dependent variation in the particular frequency that is most strongly influenced. Changes in coherence and PAC, reflecting interactions between brain regions have been shown to vary with changes in behavior in a number of different brain networks (Canolty and Knight, 2010, Siegel et al., 2012). Furthermore, some of the cortical patterns we observe in the motor system are similar to those observed in another ECoG study which examined more widespread regions of cortex (Breshears et al., 2010). However, because we focused specifically on the motor system, we cannot be sure of the generalizability of our results.

Support for the Importance of Synchronized Beta Activity in the Motor System

Converging evidence suggests that one consequence of loss of consciousness is functional disconnection between distributed brain regions (Engel and Singer, 2001, Laureys, 2005, Alkire et al., 2008, Lewis et al., 2012, Sarasso et al., 2014). For cortical and subcortical interactions, in particular, this hypothesis is supported by functional imaging studies of the recovery of awareness following traumatic unconsciousness (Goldfine and Schiff, 2011, Laureys and Schiff, 2012), and by the finding that cortical-subcortical structural connectivity correlates with levels of awareness in patients with severe head trauma (Fernandez-Espejo et al., 2011, Zheng et al., 2014). Our results support this hypothesis since two measures which reflect interactions between brain regions, coherence and cross-structure PAC, both decrease during loss of consciousness. These measures are not fully independent, since changes in coherence are likely to affect cross structure PAC.

Communication in different brain networks may occur through synchronization at particular frequencies, with the specific frequency varying depending on the brain network (Fries, 2005, Siegel et al., 2012). The motor network is dominated by activity in the alpha-beta range (Pfurtscheller, 1981, Murthy and Fetz, 1992, Sanes and Donoghue, 1993, Crone et al., 1998b, Cassidy et al., 2002, Brovelli et al., 2004, Kuhn et al., 2004, Miller et al., 2012, Yanagisawa et al., 2012). Thus, the reduction in beta coherence seen in this study would be expected to impair communication between the motor cortex and its subcortical modulators, consistent with the "communication through coherence" hypothesis (Fries, 2005). PAC provides a mechanism to explain how coherence, might influence local neural activity (Canolty et al., 2006, Canolty and Knight, 2010). Thus our observed coherence and PAC decreases are consistent with a general reduction in motor network connectivity, and perhaps communication, which can be detected with both metrics. We predict that a similar phenomenon might be observed in a different frequency range if a different brain network (with a different predominant frequency range) were studied.

Opposing Patterns of Functional Connectivity in Consciousness

Some studies, similar to our own, show a decrease in synchrony between distributed areas during loss of consciousness (Laureys et al., 1999, Bonhomme et al., 2012, Massimini et al.,

2012, Chennu et al., 2014, Sarasso et al., 2014), while others showed an increase (Feshchenko et al., 2004, Arthuis et al., 2009, Breshears et al., 2010, Ching et al., 2010, Mukamel et al., 2014). One explanation for these seemingly contradictory findings may lie in the distinction between 'healthy' synchrony, necessary to coordinate communication between separated brain areas (Fries, 2005, Siegel et al., 2012), and abnormal oscillatory pattern, which may break up normally synchronized activity or constrain neural activity in an inflexible pattern. Anesthesia may cause some populations of neurons to fire in an oscillatory, inflexible, way, which then precludes patterns of synchronization necessary for conscious behavior. Indeed, there have been studies that observe both patterns during loss of consciousness, i.e. both an increase in oscillatory activity in certain frequency ranges or brain networks, coincident with a decrease in oscillatory activity in others (Lewis et al., 2012, Purdon et al., 2013).

Alternative Interpretations of the Coherence and PAC Results

We have observed a decrease in coherence and PAC during anesthesia induction that is specific to the beta band, and not accompanied by a change in beta power in cortex (and only a general decrease in all frequencies > 20 Hz in subcortical areas.) We interpret this as a reflection of a reduction in communication throughout the motor system, which occurs specifically in beta. However, alternative interpretations are possible. For instance, the power decrease in the subcortical regions may make the subcortical phase estimate of beta less reliable, reducing coherence. We cannot rule out this interpretation, however, if this were the only factor driving the effect, we might expect more broadband coherence change, since all frequencies above 20 Hz decreased in the subcortical areas. Furthermore, this interpretation is not necessarily mutually exclusive with the hypothesis that communication at specific frequencies is decreased, since a decrease in communication could also be driven by a decrease in power at the dominant frequency for a particular structure within a brain network.

Another interpretation is that movement could have influenced the recordings, since beta is modulated by movement (Pfurtscheller, 1981, Crone et al., 1998b). While all our patients were at rest during the recordings, perhaps subtle, undetectable, movements were present in the early portions of the recording that decreased over time with anesthesia induction. However, this interpretation would predict changes opposite to those observed here (i.e. an increase in coherence with anesthesia induction), since movement has been associated with a decrease in coherence in the alpha/beta range between cortical and subcortical motor structures (Cassidy et al., 2002, Lalo et al., 2008, Alegre et al., 2010).

Changes in Power in Specific Brain Regions May Reflect Reduced Neuronal Activity or Relate to Disconnection Between Brain Regions

The propofol induced reduction in cortical broadband activity that we observed was weak, but is in general agreement with previous human studies examining ECoG during anesthesia induction (Breshears et al., 2010, Verdonck et al., 2014). The subcortical broadband gamma reduction confirms similar findings in rodent studies (Reed et al., 2013), and in one small series of thalamic recordings in humans (Verdonck et al., 2014). Broadband gamma power in cortex is thought to be an index of local neural activity and a surrogate for neural spiking

(Miller et al., 2007, Manning et al., 2009). The interpretation of broadband gamma in subcortical structures is less clear, but may similarly represent the sum of local neuronal spiking. Indeed, event-related broadband gamma changes similar to those reported in cortex have been observed in subcortical structures (Ray et al., 2012, Hamame et al., 2014).

Gamma power decreases are often associated with low frequency power increases (Crone et al., 1998a, Crone et al., 1998b). The low frequency power increases (2-6 Hz) that we observe in both cortex and subcortex may relate to this same process. Therefore, one interpretation is that the changes in power observed during loss of consciousness relate to decreased neural activity in regions that play key roles in generating behavior.

An alternative explanation is that the low frequency (2-6 Hz) power changes in both cortex and subcortex have a different etiology than the high frequency power changes. Several studies have reported low frequency power increases in cortex during anesthesia induction (Breshears et al., 2010, Lewis et al., 2012, Purdon et al., 2013, Verdonck et al., 2014). In some cases, this emerging low frequency activity is asynchronous across cortex and has been interpreted as a mechanism whereby different brain networks become disconnected from one another (Lewis et al., 2012, Purdon et al., 2013). In many of these studies, the low frequency activity is in a slightly lower frequency range (<2 Hz) than is observed here, nevertheless, other studies have shown these changes over a broader frequency range (Verdonck et al., 2014), and so it is possible that a similar mechanism is involved.

Limitations

There are several limitations to our study. While our recording methods have high temporal resolution, the precision with which the state of consciousness is assessed, using standard anesthesia scales, is less temporally precise. This may have limited the changes we could detect. All our participants were movement disorder patients, who necessarily have abnormal motor networks, and subcortical recording sites were limited to clinically indicated targets for ethical reasons. We sought to minimize this problem by including patients with different diagnoses, which presumably have different pathophysiologies, and by focusing on patterns that were consistent across patients. Nevertheless, an alternative interpretation is that activity changes associated with induction reflect the cessation of symptoms, which occurs with anesthesia. Additionally, the inclusion of different diagnoses further increased the heterogeneity of our sample, which may have decreased our sensitivity for finding effects, and makes interpretation more complex. Likewise, while examination of multiple subcortical targets allowed us to focus on motifs common to multiple nodes of the BGTC motor loop, it also increased the potential for signal variability. Thus we may be insensitive to changes that are present most strongly in only certain subcortical regions. Finally, the use of ECoG strip arrays that can be inserted via a burr hole limited our spatial sampling. Our results may not generalize to the entire cortex (although there are similarities between our data and that recorded with a greater spatial sampling, (see Breshears et al., 2010)). Investigation of other, more distributed brain networks, was precluded by the ethical constraints of working with human patients in the operating room.

Conclusion

Using a method that allowed us to simultaneously collect high spatial and temporal resolution data from human cortex and subcortical nuclei, we have shown a narrowband reduction in motor system interactions in the beta band across subjects during loss of consciousness. These results support a mechanism for communication throughout brain networks that involves synchronous oscillatory activity that is frequency-specific, and breaks down when organized recruitment of a brain network for behavior is impossible (i.e. during unconsciousness). These results shed light on possible general mechanisms of neural communication in the human brain.

Acknowledgements

References

Alegre M, Rodriguez-Oroz MC, Valencia M, Perez-Alcazar M, Guridi J, Iriarte J, Obeso JA, Artieda J. Changes in subthalamic activity during movement observation in Parkinson's disease: is the mirror system mirrored in the basal ganglia? Clin Neurophysiol. 2010; 121:414–425. [PubMed: 20006544]

Alexander GE, DeLong MR, Strick PL. Parallel organization of functionally segregated circuits linking basal ganglia and cortex. Annual review of neuroscience. 1986; 9:357–381.

Alkire, MT.; Hudetz, AG.; Tononi, G. Science. Vol. 322. New York, NY: 2008. Consciousness and anesthesia; p. 876-880.

Arthuis M, Valton L, Regis J, Chauvel P, Wendling F, Naccache L, Bernard C, Bartolomei F. Impaired consciousness during temporal lobe seizures is related to increased long-distance cortical-subcortical synchronization. Brain. 2009; 132:2091–2101. [PubMed: 19416952]

Bonhomme V, Boveroux P, Brichant JF, Laureys S, Boly M. Neural correlates of consciousness during general anesthesia using functional magnetic resonance imaging (fMRI). Archives italiennes de biologie. 2012; 150:155–163. [PubMed: 23165875]

Breshears JD, Roland JL, Sharma M, Gaona CM, Freudenburg ZV, Tempelhoff R, Avidan MS, Leuthardt EC. Stable and dynamic cortical electrophysiology of induction and emergence with propofol anesthesia. Proc Natl Acad Sci U S A. 2010; 107:21170–21175. [PubMed: 21078987]

Brovelli A, Ding M, Ledberg A, Chen Y, Nakamura R, Bressler SL. Beta oscillations in a large-scale sensorimotor cortical network: directional influences revealed by Granger causality. Proc Natl Acad Sci U S A. 2004; 101:9849–9854. [PubMed: 15210971]

Canolty, RT.; Edwards, E.; Dalal, SS.; Soltani, M.; Nagarajan, SS.; Kirsch, HE.; Berger, MS.; Barbaro, NM.; Knight, RT. Science. Vol. 313. New York, NY: 2006. High gamma power is phase-locked to theta oscillations in human neocortex; p. 1626-1628.

Canolty RT, Knight RT. The functional role of cross-frequency coupling. Trends in Cognitive Sciences. 2010; 14:506–515. [PubMed: 20932795]

Cassidy M, Mazzone P, Oliviero A, Insola A, Tonali P, Di Lazzaro V, Brown P. Movement-related changes in synchronization in the human basal ganglia. Brain. 2002; 125:1235–1246. [PubMed: 12023312]

Chennu S, Finoia P, Kamau E, Allanson J, Williams GB, Monti MM, Noreika V, Arnatkeviciute A, Canales-Johnson A, Olivares F, Cabezas-Soto D, Menon DK, Pickard JD, Owen AM, Bekinschtein TA. Spectral signatures of reorganised brain networks in disorders of consciousness. PLoS computational biology. 2014; 10:e1003887. [PubMed: 25329398]

Chernik DA, Gillings D, Laine H, Hendler J, Silver JM, Davidson AB, Schwam EM, Siegel JL. Validity and reliability of the Observer's Assessment of Alertness/Sedation Scale: study with

intravenous midazolam. Journal of clinical psychopharmacology. 1990; 10:244–251. [PubMed: 2286697]

Ching S, Cimenser A, Purdon PL, Brown EN, Kopell NJ. Thalamocortical model for a propofol-induced alpha-rhythm associated with loss of consciousness. Proc Natl Acad Sci U S A. 2010; 107:22665–22670. [PubMed: 21149695]

Crone NE, Miglioretti DL, Gordon B, Lesser RP. Functional mapping of human sensorimotor cortex with electrocorticographic spectral analysis. II. Event-related synchronization in the gamma band. Brain. 1998a; 121:2301–2315. Pt 12. [PubMed: 9874481]

Crone NE, Miglioretti DL, Gordon B, Sieracki JM, Wilson MT, Uematsu S, Lesser RP. Functional mapping of human sensorimotor cortex with electrocorticographic spectral analysis. I. Alpha and beta event-related desynchronization. Brain. 1998b; 121:2271–2299. Pt 12. [PubMed: 9874480]

Crowell AL, Ryapolova-Webb ES, Ostrem JL, Galifianakis NB, Shimamoto S, Lim DA, Starr PA. Oscillations in sensorimotor cortex in movement disorders: an electrocorticography study. Brain. 2012

de Hemptinne C, Ryapolova-Webb ES, Air EL, Garcia PA, Miller KJ, Ojemann JG, Ostrem JL, Galifianakis NB, Starr PA. Exaggerated phase-amplitude coupling in the primary motor cortex in Parkinson disease. Proc Natl Acad Sci U S A. 2013; 110:4780–4785. [PubMed: 23471992]

de Hemptinne C, Swann N, Ostrem J, Ryapolova-Webb E. Therapeutic deep brain stimulation reduces cortical phase amplitude coupling in Parkinson's disease. Nat Neurosci. 2015 M SL, N G, P S. in press.

Delorme A, Makeig S. EEGLAB: an open source toolbox for analysis of single-trial EEG dynamics including independent component analysis. Journal of neuroscience methods. 2004; 134:9–21. [PubMed: 15102499]

Engel AK, Singer W. Temporal binding and the neural correlates of sensory awareness. Trends Cogn Sci. 2001; 5:16–25. [PubMed: 11164732]

Fechner J, Ihmsen H, Hatterscheid D, Jeleazcov C, Schiessl C, Vornov JJ, Schwilden H, Schuttler J. Comparative pharmacokinetics and pharmacodynamics of the new propofol prodrug GPI 15715 and propofol emulsion. Anesthesiology. 2004; 101:626–639. [PubMed: 15329587]

Fernandez-Espejo D, Bekinschtein T, Monti MM, Pickard JD, Junque C, Coleman MR, Owen AM. Diffusion weighted imaging distinguishes the vegetative state from the minimally conscious state. Neuroimage. 2011; 54:103–112. [PubMed: 20728553]

Feshchenko VA, Veselis RA, Reinsel RA. Propofol-induced alpha rhythm. Neuropsychobiology. 2004; 50:257–266. [PubMed: 15365226]

Follett KA, Weaver FM, Stern M, Hur K, Harris CL, Luo P, Marks WJ Jr. Rothlind J, Sagher O, Moy C, Pahwa R, Burchiel K, Hogarth P, Lai EC, Duda JE, Holloway K, Samii A, Horn S, Bronstein JM, Stoner G, Starr PA, Simpson R, Baltuch G, De Salles A, Huang GD, Reda DJ, Group CSPS. Pallidal versus subthalamic deep-brain stimulation for Parkinson's disease. The New England journal of medicine. 2010; 362:2077–2091. [PubMed: 20519680]

Fries P. A mechanism for cognitive dynamics: neuronal communication through neuronal coherence. Trends in Cognitive Sciences. 2005; 9:474–480. [PubMed: 16150631]

Goldfine AM, Schiff ND. Consciousness: its neurobiology and the major classes of impairment. Neurologic clinics. 2011; 29:723–737. [PubMed: 22032656]

Hamame CM, Alario FX, Llorens A, Liegeois-Chauvel C, Trebuchon-Da Fonseca A. High frequency gamma activity in the left hippocampus predicts visual object naming performance. Brain and language. 2014; 135:104–114. [PubMed: 25016093]

Kuhn AA, Williams D, Kupsch A, Limousin P, Hariz M, Schneider GH, Yarrow K, Brown P. Event-related beta desynchronization in human subthalamic nucleus correlates with motor performance. Brain. 2004; 127:735–746. [PubMed: 14960502]

Lalo E, Thobois S, Sharott A, Polo G, Mertens P, Pogosyan A, Brown P. Patterns of bidirectional communication between cortex and basal ganglia during movement in patients with Parkinson disease. J Neurosci. 2008; 28:3008–3016. [PubMed: 18354004]

Laureys S. The neural correlate of (un)awareness: lessons from the vegetative state. Trends Cogn Sci. 2005; 9:556–559. [PubMed: 16271507]

Laureys S, Goldman S, Phillips C, Van Bogaert P, Aerts J, Luxen A, Franck G, Maquet P. Impaired effective cortical connectivity in vegetative state: preliminary investigation using PET. Neuroimage. 1999; 9:377–382. [PubMed: 10191166]

Laureys S, Schiff ND. Coma and consciousness: paradigms (re)framed by neuroimaging. Neuroimage. 2012; 61:478–491. [PubMed: 22227888]

Lewis LD, Weiner VS, Mukamel EA, Donoghue JA, Eskandar EN, Madsen JR, Anderson WS, Hochberg LR, Cash SS, Brown EN, Purdon PL. Rapid fragmentation of neuronal networks at the onset of propofol-induced unconsciousness. Proc Natl Acad Sci U S A. 2012; 109:E3377–3386. [PubMed: 23129622]

Manning JR, Jacobs J, Fried I, Kahana MJ. Broadband shifts in local field potential power spectra are correlated with single-neuron spiking in humans. J Neurosci. 2009; 29:13613–13620. [PubMed: 19864573]

Massimini M, Ferrarelli F, Sarasso S, Tononi G. Cortical mechanisms of loss of consciousness: insight from TMS/EEG studies. Archives italiennes de biologie. 2012; 150:44–55. [PubMed: 23165870]

Miller KJ, Hermes D, Honey CJ, Hebb AO, Ramsey NF, Knight RT, Ojemann JG, Fetz EE. Human motor cortical activity is selectively phase-entrained on underlying rhythms. PLoS computational biology. 2012; 8:e1002655. [PubMed: 22969416]

Miller KJ, Leuthardt EC, Schalk G, Rao RPN, Anderson NR, Moran DW, Miller JW, Ojemann JG. Spectral Changes in Cortical Surface Potentials during Motor Movement. Journal of Neuroscience. 2007; 27:2424–2432. [PubMed: 17329441]

Mukamel EA, Pirondini E, Babadi B, Wong KF, Pierce ET, Harrell PG, Walsh JL, Salazar-Gomez AF, Cash SS, Eskandar EN, Weiner VS, Brown EN, Purdon PL. A transition in brain state during propofol-induced unconsciousness. J Neurosci. 2014; 34:839–845. [PubMed: 24431442]

Murthy VN, Fetz EE. Coherent 25-to 35-Hz oscillations in the sensorimotor cortex of awake behaving monkeys. Proc Natl Acad Sci U S A. 1992; 89:5670–5674. [PubMed: 1608977]

Papavassiliou E, Rau G, Heath S, Abosch A, Barbaro NM, Larson PS, Lamborn K, Starr PA. Thalamic deep brain stimulation for essential tremor: relation of lead location to outcome. Neurosurgery. 2004; 54:1120–1129. discussion 1129-1130. [PubMed: 15113466]

Pfurtscheller G. Central beta rhythm during sensorimotor activities in man. Electroencephalogr Clin Neurophysiol. 1981; 51:253–264. [PubMed: 6163614]

Purdon PL, Pierce ET, Mukamel EA, Prerau MJ, Walsh JL, Wong KF, Salazar-Gomez AF, Harrell PG, Sampson AL, Cimenser A, Ching S, Kopell NJ, Tavares-Stoeckel C, Habeeb K, Merhar R, Brown EN. Electroencephalogram signatures of loss and recovery of consciousness from propofol. Proc Natl Acad Sci U S A. 2013; 110:E1142–1151. [PubMed: 23487781]

Ray NJ, Brittain JS, Holland P, Joundi RA, Stein JF, Aziz TZ, Jenkinson N. The role of the subthalamic nucleus in response inhibition: Evidence from local field potential recordings in the human subthalamic nucleus. Neuroimage. 2012; 60:271–278. [PubMed: 22209815]

Raz A, Eimerl D, Zaidel A, Bergman H, Israel Z. Propofol decreases neuronal population spiking activity in the subthalamic nucleus of Parkinsonian patients. Anesthesia and analgesia. 2010; 111:1285–1289. [PubMed: 20841416]

Reed SJ, Plourde G, Tobin S, Chapman CA. Partial antagonism of propofol anaesthesia by physostigmine in rats is associated with potentiation of fast (80-200 Hz) oscillations in the thalamus. British journal of anaesthesia. 2013; 110:646–653. [PubMed: 23213035]

Sanes JN, Donoghue JP. Oscillations in local field potentials of the primate motor cortex during voluntary movement. Proc Natl Acad Sci U S A. 1993; 90:4470–4474. [PubMed: 8506287]

Sarasso S, Rosanova M, Casali AG, Casarotto S, Fecchio M, Boly M, Gosseries O, Tononi G, Laureys S, Massimini M. Quantifying cortical EEG responses to TMS in (un)consciousness. Clinical EEG and neuroscience. 2014; 45:40–49. [PubMed: 24403317]

Shahlaie K, Larson PS, Starr PA. Intraoperative computed tomography for deep brain stimulation surgery: technique and accuracy assessment. Neurosurgery. 2011; 68:114–124. discussion 124. [PubMed: 21206322]

Shimamoto SA, Ryapolova-Webb ES, Ostrem JL, Galifianakis NB, Miller KJ, Starr PA. Subthalamic nucleus neurons are synchronized to primary motor cortex local field potentials in Parkinson's disease. J Neurosci. 2013; 33:7220–7233. [PubMed: 23616531]

Siegel M, Donner TH, Engel AK. Spectral fingerprints of large-scale neuronal interactions. Nat Rev Neurosci. 2012; 13:121–134. [PubMed: 22233726]

Smith C, McEwan AI, Jhaveri R, Wilkinson M, Goodman D, Smith LR, Canada AT, Glass PS. The interaction of fentanyl on the Cp50 of propofol for loss of consciousness and skin incision. Anesthesiology. 1994; 81:820–828. discussion 826A. [PubMed: 7943832]

Starr PA, Christine CW, Theodosopoulos PV, Lindsey N, Byrd D, Mosley A, Marks WJ Jr. Implantation of deep brain stimulators into the subthalamic nucleus: technical approach and magnetic resonance imaging-verified lead locations. Journal of neurosurgery. 2002; 97:370–387. [PubMed: 12186466]

Starr PA, Turner RS, Rau G, Lindsey N, Heath S, Volz M, Ostrem JL, Marks WJ Jr. Microelectrode-guided implantation of deep brain stimulators into the globus pallidus internus for dystonia: techniques, electrode locations, and outcomes. Journal of neurosurgery. 2006; 104:488–501. [PubMed: 16619651]

Tort AB, Kramer MA, Thorn C, Gibson DJ, Kubota Y, Graybiel AM, Kopell NJ. Dynamic cross-frequency couplings of local field potential oscillations in rat striatum and hippocampus during performance of a T-maze task. Proc Natl Acad Sci U S A. 2008; 105:20517–20522. [PubMed: 19074268]

van Wijk BC, Beek PJ, Daffertshofer A. Neural synchrony within the motor system: what have we learned so far? Frontiers in human neuroscience. 2012; 6:252. [PubMed: 22969718]

Verdonck O, Reed SJ, Hall J, Gotman J, Plourde G. The sensory thalamus and cerebral motor cortex are affected concurrently during induction of anesthesia with propofol: a case series with intracranial electroencephalogram recordings. Canadian journal of anaesthesia = Journal canadien d'anesthesie. 2014; 61:254–262.

Yanagisawa T, Yamashita O, Hirata M, Kishima H, Saitoh Y, Goto T, Yoshimine T, Kamitani Y. Regulation of motor representation by phase-amplitude coupling in the sensorimotor cortex. J Neurosci. 2012; 32:15467–15475. [PubMed: 23115184]

Yousry TA, Schmid UD, Alkadhi H, Schmidt D, Peraud A, Buettner A, Winkler P. Localization of the motor hand area to a knob on the precentral gyrus. A new landmark. Brain. 1997; 120:141–157. Pt 1. [PubMed: 9055804]

Zheng Z, Reggente N, Lutkenhoff E, Owen AM, Monti M. Structural connectivity between the thalamus and fronto-temporal regions predicts level of awareness in disorders of consciousness. Society for Neuroscience Conference (Abs). 2014

Author Manuscript

Author Manuscript

Author Manuscript

Author Manuscript
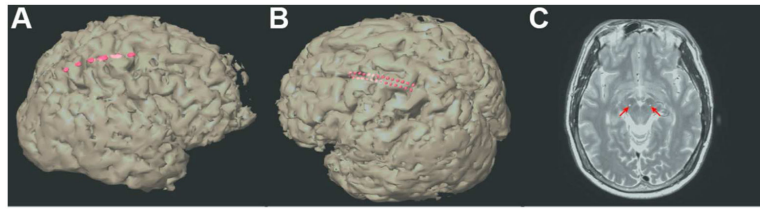
1.

3D brain reconstructions of each subject's MRI with the low resolution (**A**) and high resolution (**B**) ECoG strips, and the subcortical DBS electrode, positioned in STN (indicated with red arrows) **(C)**. Electrode locations (shown in red) are visualized by merging an intraoperative CT with a preoperative MRI.
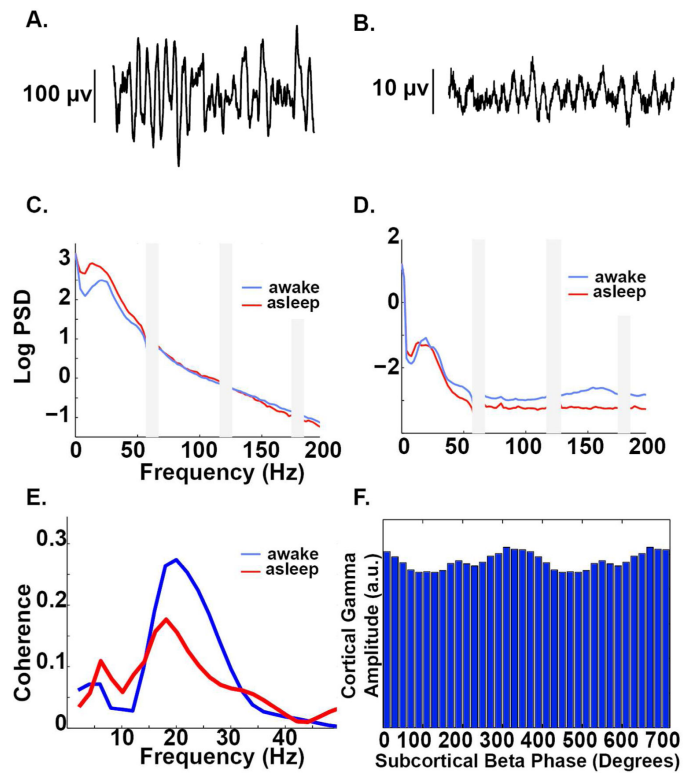
2.

Example data from individual subject #6. One second of raw M1 ECoG **(A)** data and raw LFP data (from STN) **(B)**. Log PSD from M1 **(C)** and STN **(D)**. The gray bars indicate 60 Hz noise and the harmonics. **(E)** Coherence between M1 and STN **(F)**. Histogram of mean M1 broadband gamma amplitude (70-150 Hz) binned by subcortical beta phase (18-20 Hz). Here modulation is apparent. A flat distribution would suggest no PAC.
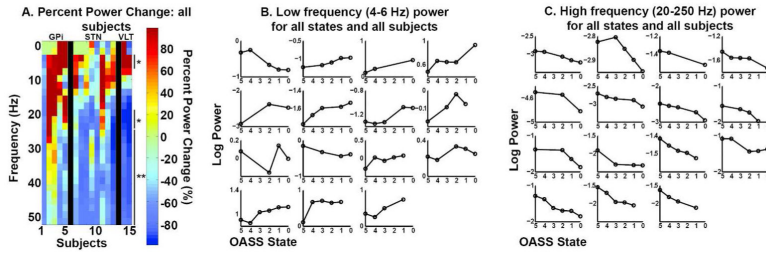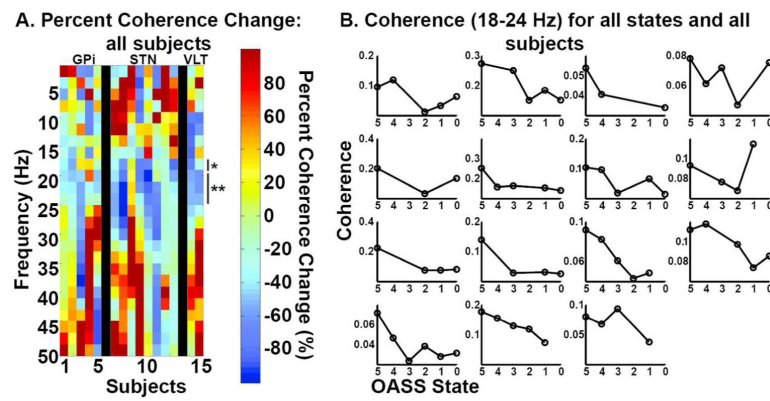
3.

Subcortical power changes. **A**. Percent power change for all frequencies and subjects. Percent change was calculated as: ((asleep-awake)/ awake)*100. Significant differences are indicated with one (p<0.05, FDR corrected) or two asterisks (p<0.01, FDR corrected). Subjects are grouped by region of LFP recordings, indicated with labels (i.e. GPi, STN, and ventrolateral thalamus (VLT)) and separated by black bars. Subject 1 was the dystonia patient, subjects 2-5 and 6-13 were PD patients, and subjects 14-15 were ET patients. To be consistent with subsequent figures, only frequencies below 50 Hz are shown, although higher frequencies were analyzed and described in C. **B**. Individual subject log power for each state averaged across the frequencies with a significant increase in power (4-6 Hz). Subject order is the same as in A, with subjects 1-4 making up the first row. **C**. Same as B, but showing average log power for all frequencies with a significant decrease during induction (20-250 Hz).
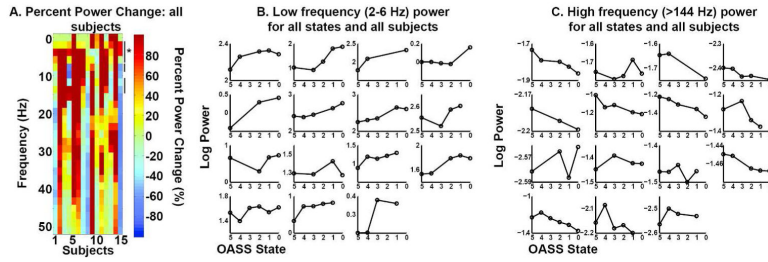
4.

M1 power changes. **A** Same as Figure 3A, except M1 power changes. To be consistent with subsequent figures, only frequencies up to 50 Hz are shown, although higher frequencies were analyzed and described in C. The asterisk indicates significant frequencies ($p<0.05$, FDR corrected), and the line without an asterisk indicates significance at $p<0.05$, uncorrected. Subjects 1, 2, 3, 6, 7, and 8 were recorded with the low-resolution grid. The others were recorded with the high-resolution grid. **(B-C)** Same as 3B-C except showing values M1 power changes for frequencies with a significant increase **(B,** 2-6 Hz, $p<0.05$, FDR corrected) and **(C)** significant decrease (> 144 Hz, $p<0.05$, uncorrected).

A. Percent Coherence Change: all subjects

B. Coherence (18-24 Hz) for all states and all subjects

5.

M1 and subcortical coherence changes. **A**. Same as Figure 3A, except M1 and subcortical coherence changes. Significant differences are indicated with one (p<0.05, FDR corrected) or two asterisks (p<0.01, FDR corrected). **B.** Individual subject coherence shown for each state for 18-24 Hz. Subject order is the same as in Figure 3B.

A. Percent PAC Change: all subjects

B. PAC (18-20 Hz) for all states and all subjects
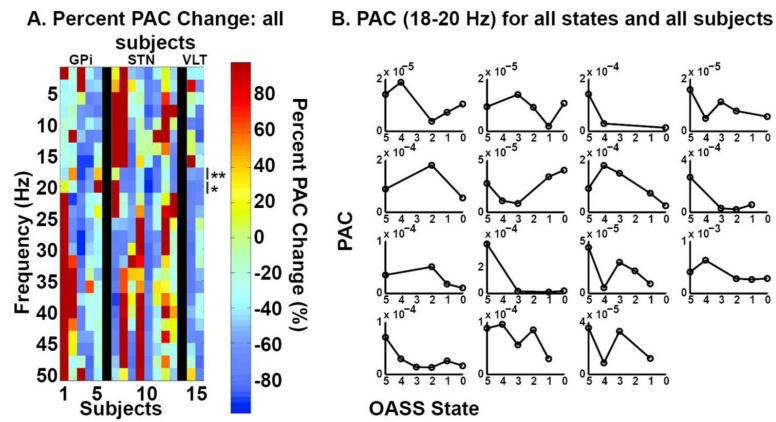
6.

M1 and subcortical PAC changes. PAC is calculated using subcortical phase and broadband M1 amplitude (70-150 Hz). **A**. Same as Figure 3A, except PAC changes. Significant differences are indicated with one ($p<0.05$, FDR corrected) or 2 asterisks ($p<0.01$, FDR corrected). **B.** Individual subject PAC averaged between 18-20 Hz. Subject order is the same as in Figure 3B.

Table 1

MOAA/S Responsiveness Scale. Rating criteria for each state.

State	Responsiveness
5	Responds readily to name spoken in normal tone
4	Lethargic response to name spoken in normal tone
3	Responds only after name is called loudly and/or repeatedly
2	Responds only after mild prodding or shaking
1	Responds only after painful trapezius squeeze
0	No response after painful trapezius squeeze